Supporting Information For

Influence of the functionalization of nanocontainers on the self-healing anticorrosive coatings

Zhaoliang Zheng[†,*], Matthias Schenderlein[‡], Xing Huang,[§] Nick J. Brownbill[†], Frédéric Blanc[†] and Dmitry Shchukin[†]

[†]Stephenson Institute for Renewable Energy, Department of Chemistry, University of Liverpool, Crown Street, Liverpool, L69 7ZD, UK.

E-mail: zhaoliang.zheng@liverpool.ac.uk

[‡]Max-Planck Institute of Colloids and Interfaces, 14424, Potsdam, Germany.

[§]Fritz-Haber-Institut der MPG, Faradayweg 4-6, 14195, Berlin, Germany.

1. Materials and Reagents

Tetraethyl orthosilicate (TEOS, reagent grade, 98%), sodium hydroxide solution (~1.0 M NaOH), hexadecyltrimethylammonium bromide (≥98%), toluene (anhydrous, 99.8%), N-[3-(Trimethoxysilyl)propyl]ethylenediamine (97%), methyl sulfoxide (≥99%), succinic anhydride (97%), Triethylamine (≥99%), 1*H*-benzotriazole (≥98.0%), cobalt(II) nitrate hexahydrate (ACS reagent, ≥98%), copper(II) sulfatepentahydrate (ACS reagent, ≥98.0%) and sodium carbonate (99.95-100.05% dry basis) were all purchased from Sigma-Aldrich. (trimethoxysilylpropyl)-ethylenediaminetriacetic acid trisodium salt (45% in water) was bought from ABCR GmbH & CO. KG.

2. Synthetic procedure

MCM-41 nanoparticles. MCM-41 nanoparticles were fabricated according to the method reported.[1] Briefly, 950 mL of deionized water, 2 g of hexadecyltrimethylammonium bromide and 14 mL of sodium hydroxide solution (~1.0 M NaOH) were mixed and preheated at 80 °C for 1 h. Then 10 mL of TEOS was dropped in within 30 min. The mixture was further heated for 2 hours and followed by an ambient cooling. The template can be removed by calcination at 550 °C for 3 h in air.

en-MCM-41. The bared mesoporous silica solid (2 g) was dispersed in 500 mL of dry toluene to which 0.14 mL (for 0.7 mmol/g) or 0.05 mL (for 0.2 mmol/g) of N-[3-(Trimethoxysilyl) propyl]ethylenediamine was added. The mixed solution was continuously stirred at 120 °C for 20 h resulting in MCM-41 functionalized with en-type agent. The product was dried in vacuum oven at 60 °C overnight.

en-$(COO^-)_3$-MCM-41. This compound was prepared as described for **en-MCM-41** using 0.6 mL (for 0.7 mmol/g) or 0.14 mL (for 0.2 mmol/g) of (trimethoxysilylpropyl)-ethylenediaminetriacetic acid trisodium salt aqueous solution as silane source. The drying step was similar with the above mentioned.

en-(COO^-)-MCM-41. The **en-MCM-41** powder (2 g) was dispersed in 50 mL of DMSO to which 43 μL of triethylamine and 600 mg (for 0.7 mmol/g) or 200 mg (for 0.2 mmol/g) of succinic anhydride was added. The stoichiometry of the succinic anhydride vs attached en moiety was around 4. The mixed solution was continuously stirred at 40 °C for 48 h, resulting in en-(COO^-)-MCM-41. The resulting product was washed with DMSO and ethanol, and then dried in vacuum oven at 60 °C overnight.

3. Loading procedure

The subsequent loading of the silica containers with cargo molecules was conducted under reduced pressure (30 mbar) for three times. Afterwards, the as-loaded containers were separated by filtration and further cleaned by method developed by us.[2] For example, to obtain "clean" loaded nanocontainers without surface absorbed 1*H*-benzotriazole (BTA), a quick washing method was needed to prevent spontaneous leakage of the loaded active compounds. A home-made washing device was simply composed of a piece of filter paper with a mesh at 0.05 μm, a funnel and a pump. Before washing, a thin layer of freshly-loaded containers powder was made on the filter paper by careful pressing with a chemical spoon. Then water was dropped on the layer and removed by the funnel connected with the pump. The procedure was stopped till the washed-out BTA (determined by UV analysis) remained neglectible.

4. Formation of nanovalves

After washing and drying, a sprayer was used for forming nanovalves on the loaded containers in a large amount. Typically, 0.1 M $Co(NO_3)_2$ solution was sprayed on the powders, which was followed by removing excess salt using a similar technique for washing away the surface-absorbed BTA. The same amount of 0.2 M Na_2CO_3 solution was then sprayed. The resulting products were sealed for 3-days aging and then introduced in coating matrix[3] for self-healing anticorrosion.

5. Surface functionalization of silicon wafers

The wafers were cleaned with piranha solution of H_2SO_4/H_2O_2 (7/3 volume ratio) at 90 °C for 60 min.

For en-functionalization, the solution (10 mL) containing 75% water and 25% methanol was mixed with 700 µL and 200 µL of N-[3-(Trimethoxysilyl)propyl]ethylenediamine, respectively. For en-$(COO^-)_3$-functionalization, 1 mL and 400 µL of (trimethoxysilylpropyl)-ethylenediaminetriacetic acid trisodium salt aqueous solution were added, respectively. The pH value of solution was tuned by acetic acid to 4.5. The mixtures were allowed to be still for the hydrolysis of alkoxide.

The wafers were then immersed in the solutions for 30 min. After rinsing with water/methanol mixture, they were cured at 110 °C for another 30 min.

The en-functionalized wafers were further immersed in DMSO (10 mL) containing 10 µL of triethylamine and 120 mg (for 0.7 mmol/g) or 40 mg (for 0.2 mmol/g) of succinic anhydride for en-(COO^-)-functionalized wafer. After heating at 40 °C for 12 h, the en-(COO^-)-functionalized wafer was rinsing with water/methanol mixture.

6. Coatings procedure

The water-based organic coating is a two-component, model coating developed as a primer for aerospace applications by Mankiewicz GmbH. The resin component is an epoxy based primer which consists of synthetic resins and water. The hardener component consists of polyamines in water. Water suspensions of the BTA or capped loaded FSNs were added to the pre-mixed two components under stirring. The amount of water used to redisperse the containers prior to mixing with the paint was only 5 wt% of the paint and had no detrimental effect on the paint formulation. The samples were coated on the AA2024-T3 aluminium alloy plates (scrubbed clean with NaOH, then nitric acid) using a Bungard RDC 15 dip coater (immersion time 5 min) and dried at 80 °C for 1 h after a flash-off time of 15 min at room temperature.

7. Structure characterization

HADDF STEM image and STEM EDX mapping were recorded from Cs–corrected Titan 80–300 microscopes operated at 300 kV. TEM (Zeiss EM912) were used to characterize the structure of the samples.

BET (Macromeritics TriStar 3000 system), DLS (Malvern Zetasizer 4), SEM (Hitachi S-4800) and optical microscopy were also utilized. Small-angle X-ray scattering (SAXS) measurements were performed on a Kratky camera from Anton Paar Instruments (wavelength 0.154 nm).

All solid-state NMR experiments were performed on a 400 MHz 9.4 T Bruker Avance III HD solid-state NMR spectrometer equipped with a 4 mm HXY triple-resonance magic angle spinning (MAS) probe (in double resonance mode) tuned to ^{13}C at $\nu_o(^{13}C)$ = 100.03 MHz. All experiments were performed at room temperature under MAS at ν_r = 12.5 kHz. ^{1}H pulses and SPINAL-64 heteronuclear decoupling[4] were performed at a radio-frequency (rf) field amplitude of 83 kHz. ^{1}H-^{13}C cross polarisation (CP) MAS experiments were obtained with a ^{13}C rf field of 45 kHz, while the ^{1}H rf field amplitude was ramped to obtain maximum signal at a ^{1}H rf field of approximately 60 kHz, and a contact time of 2 ms. 28 – 108 k scans were accumulated with a 3 – 4 s recycle delay. The ^{13}C chemical shifts were referenced to the CH carbon of adamantane at 29.45 ppm.[5]

Thermogravimetric analysis (TGA) was performed on Netzsch TG 209 F1 at a scanning rate of 20 K/min under a nitrogen atmosphere. The organic molar contents were estimated according to the following equations:

FSNs 1 and FSNs 2:

$$Content\left(H_{13}N_2C_5\right) = \frac{\frac{w\left(H_{13}N_2C_5\right)}{M\left(H_{13}N_2C_5\right)}}{w_0},$$

where $w(H_{13}N_2C_5)$, determined by TGA, represents the weight of organic moiety in en-MCM-41 samples; $M(H_{13}N_2C_5)$ is molar weight of the organic modification; w_0 is the weight of dry TGA samples.

For FSNs 3 and FSNs 4, the organic molar contents were calculated with $M(H_{16}O_3N_2C_9)$. Finally, $M(H_{16}O_6N_2C_{11})$ will be used in the case of FSNs 5 and FSNs 6.

Static water contact angle values were determined with a Krüss contact angle measuring system (G10). AFM images of the coatings were recorded in air at room temperature using a Nanoscope III Multimode SFM (Digital Instruments, Inc., Santa Barbara, U.S.A.).

UV-vis spectroscopy (8453 UV-visible spectrophotometer, Agilent technologies) was applied to determine the release profile of BTA. The 1 mg powder was placed in the bottom of a small bag which is made of a screen mesh membrane with mesh at around 1 μm. Then, buffer solution (at pH ≈ 7, 4 mL) was added to the cuvette till the bottom of the bag was immersed into water. A 5-mm stirring bar was added to the cuvette. The solution in the cuvette was stirred vigorously to quickly balance the concentration of the releasing BTA. The UV detector focuses into the solution at 2 cm above the bottom and around 1 cm below the top of the cuvette. The absorbance of BTA at 275 nm was plotted as a function of time in order to generate a release profile. The final concentration of BTA was determined by UV spectroscopy. Stimulated release of BTA from the containers was accomplished by changing the neutral solution with the one with lower pH value.

Scratches were made with a circular-edge scalpel without spoiling the metal surface. The scalpel was immobilized at a home-made device which can tune the loading weight in order to obtain the defect area with a suitable size. The defect area in our work is ≈ 2 mm long, 20 μm wide and ≈ 50 μm deep. For the characterization and quantification of the corrosion process in dip-coated Al alloy substrates, scanning vibrating electrode technique (SVET) and the

impedance spectroscopy (EIS, Ivium technologies) were employed. Detailed information can be seen in previous papers of our group.[6]

8. Analysis for pH sensitive release

The nanovalves formed by quick reaction between $Co(NO_3)_2$ (0.1 M) and Na_2CO_3 (0.2 M) can respond to pH lowering by gradual dissolution of the valve structure. Furthermore, the 3D porous nanovalve provides a large number of unsheltered Co^{2+}centers due to the amorphous state and the relatively large surface area, which also facilitates the strong complexation with BTA. Such complex bonds usually deform in response to a pH lowering due to the protonation of electron donating agents. Thus, the controlled release system that is sensitive to acidity of bulk solution can be constructed with inherent pH-sensitivity of the cobalt basic carbonate nanovalve and complex bonds.[7]

At the same time, considering the electrostatic repulsion between negatively charged carboxylate groups and guest molecules (BTA) in basic environment, which was actually reported to cease the release of cargo,[8] we prefer the mechanism that the silica structure was dissolved in the presence of OH^- attack. For example, the mesoporous structure of **FSNs 5** cannot be maintained after base-stimulated release measurement, as shown in Figure S9.

Table S1: ^{13}C chemical shifts and spectral assignements for FSNs.

FSNs	δ_{iso} / ppm	^{13}C NMR assignments
FSNs 2 en-MCM-41	9	Si*C*H_2-
	22	SiCH_2*C*H_2-
	40	-*C*$H_2$$NH_2$
	51	-NH*C*$H_2$$CH_2$$NH_2$
	59	-Si$CH_2$$CH_2$*C*$H_2$NH-
FSNs 4 en-(COO^-)-MCM-41	8	Si*C*H_2-
	21	SiCH_2*C*H_2-
	29	-CO*C*H_2-
	37	-*C*H_2NHCO-
	47	-*C*$H_2$$COO^-$
	50	-NH*C*$H_2$$CH_2$NHCO-
	59	-Si$CH_2$$CH_2$*C*$H_2$-
	175	-NH*C*OCH_2
	180	-*C*OO^-
FSNs 6 en-(COO^-)$_3$-MCM-41	11	Si*C*H_2-
	19	SiCH_2*C*H_2-
	55	-*C*H_2N($CH_2$$COO^-$)$_2$
	59	-*C*$H_2$$CH_2$N($CH_2$$COO^-$)$_2$ Si$CH_2$$CH_2$*C*$H_2$-
	61	-N(*C*$H_2$$COO^-$)$_2$
	63	-(CH_2)$_2$N*C*$H_2$$COO^-$
	176	-*C*OO^-

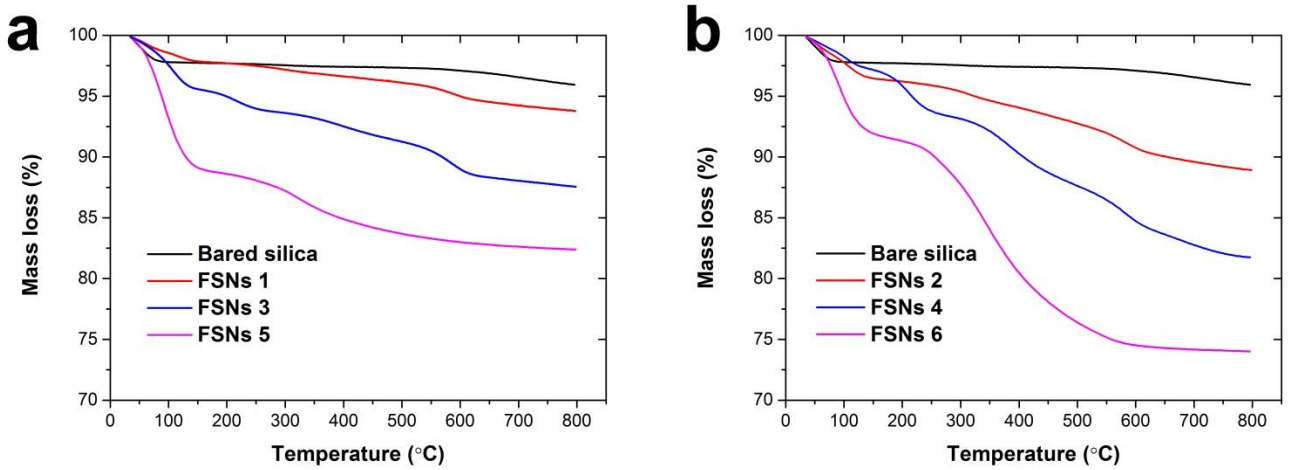

Figure S1. Thermogravimetric data for (a) bared silica, **FSNs 1**, **3** and **5**, and (b) **FSNs 2**, **4** and **6**. Here, **FSNs 1**, **3** and **5** refer the mesoporous silica nanoparticles with low organosilyl coverage (around 0.2 mmol/g) with terminal en-, en-(COO^-)- and en-($COO^-)_3$- moieties. **FSNs 2**, **4** and **6** represent the higher one (around 0.7 mmol/g).

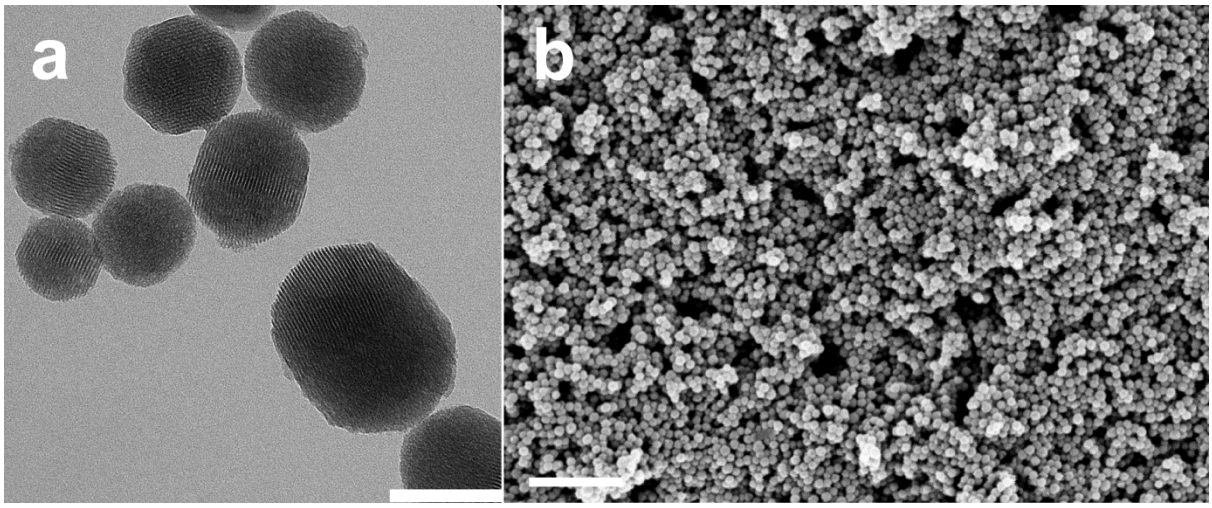

Figure S2. TEM (a) and SEM (b) images of MCM-41 nanoparticles. TEM scale bar: 100 nm. SEM scale bar: 1μm.

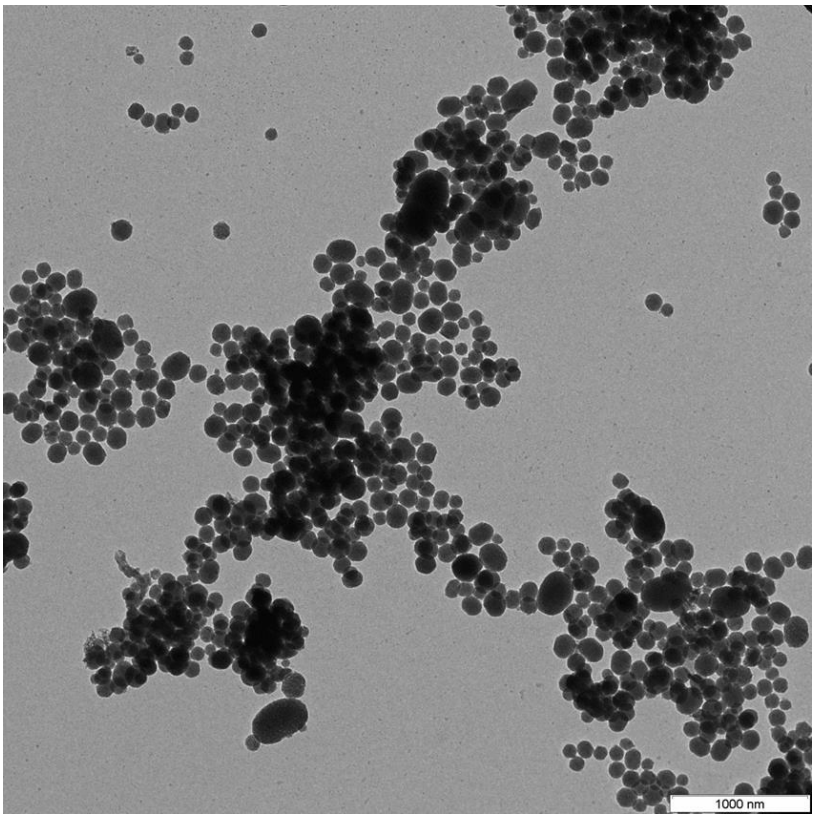

Figure S3. TEM image of **FSNs 6** made with high dose en-$(COO^-)_3$-functionalizing agent.

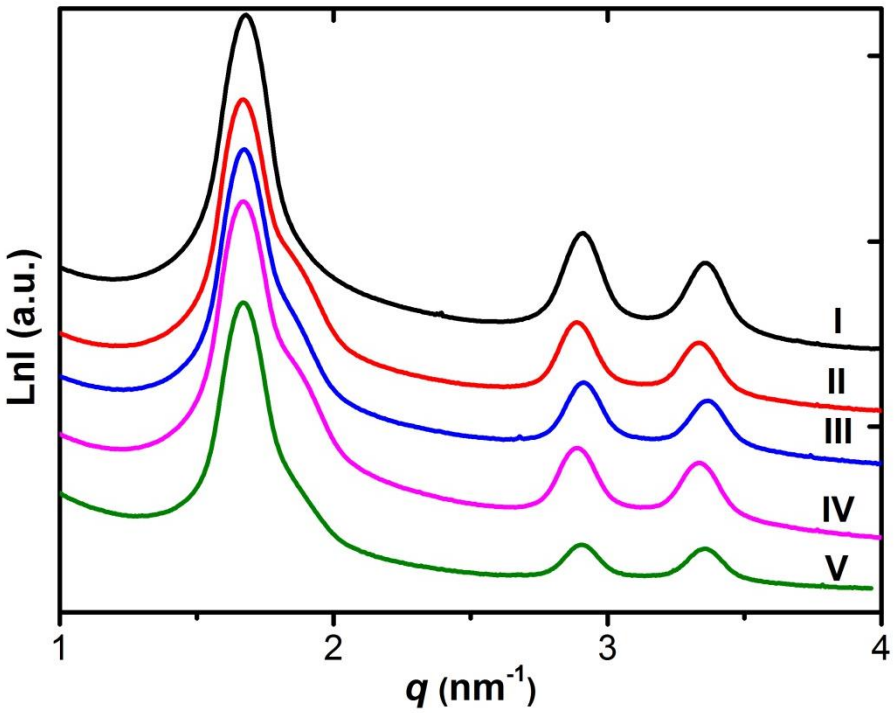

Figure S4. SAXS spectra of native MCM-41 (I), **FSNs 2** (II), **FSNs 1** (III), **FSNs 4** (IV) and **FSNs 3** (V).

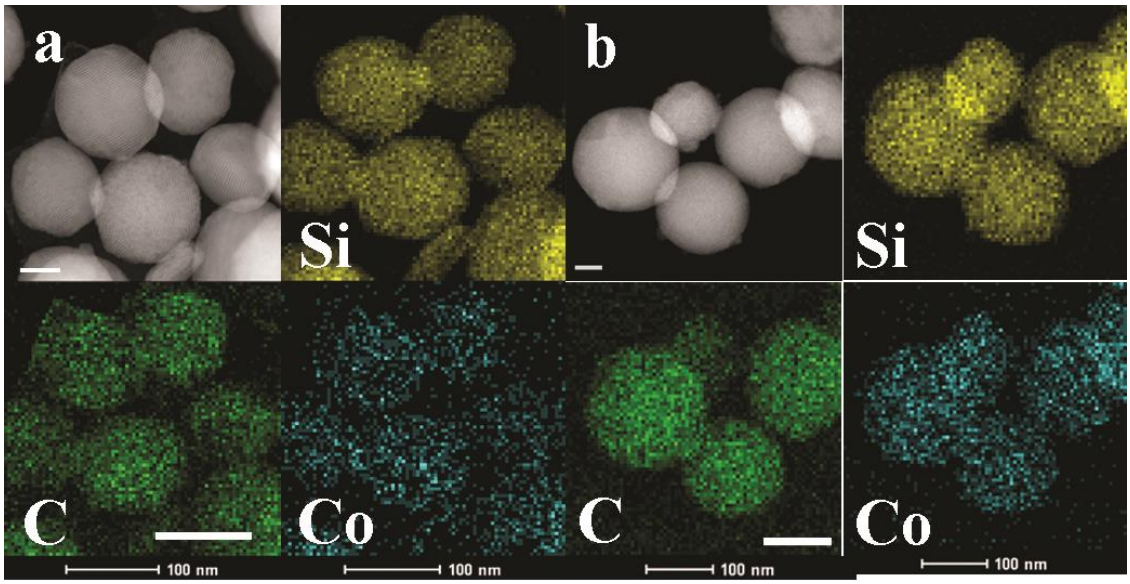

Figure S5. HAADF-STEM and elemental mapping image of loaded **FSNs 4** (a) and **FSNs 5** (b) with Co-Carbonate nanovalves. Silicon, carbon and cobalt element mapping are presented. Scale bar: HAADF-STEM 50 nm, elemental mapping 100 nm.

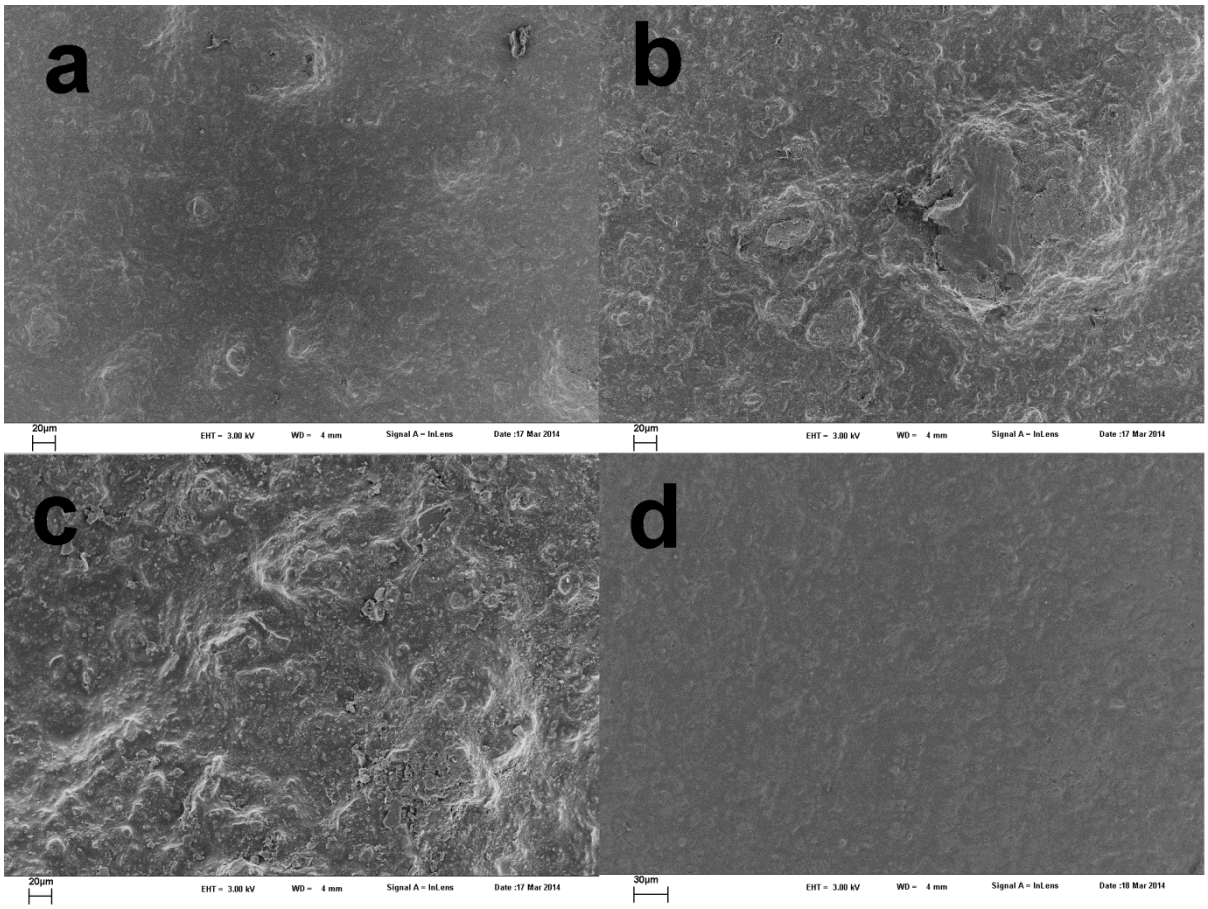

Figure S6. Top view SEM images of surface morphology of hybrid coatings containing (a) pure epoxy coating, coating containing capped loaded (b) **FSNs 2**, (c) **FSNs 4** and (d) **FSNs 5**.

The surface morphologies of the hybrid coatings are shown in Figure S6. The smoothest coating surface can be obtained by introducing capped loaded **FSNs 5** into the coating matrix, where no obvious cracks and bulges are detected (Figure S6d). This indicates the good dispersibility of the nanocontainers in the coating matrix. But defects appear as the capped loaded **FSNs 4** and **FSNs 2** are incorporated, as shown in Figure S6b-c. Notable defects on the coating surface can also be detected even by naked eyes.

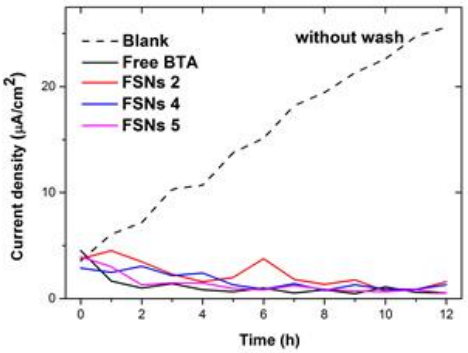

Figure S7. Maximum anodic currents detected with SVET over the scanned scratched area during a 12 h immersion period in 0.1 M NaCl. Results are shown for samples coated with an epoxy coating containing nothing, free inhibitor, capped loaded **FSNs 2**, **FSNs 4** and **FSNs 5**. The measurement was conducted without pre-wash with a flowing artificial seawater environment for 1 hour to remove free or leaked inhibitors.

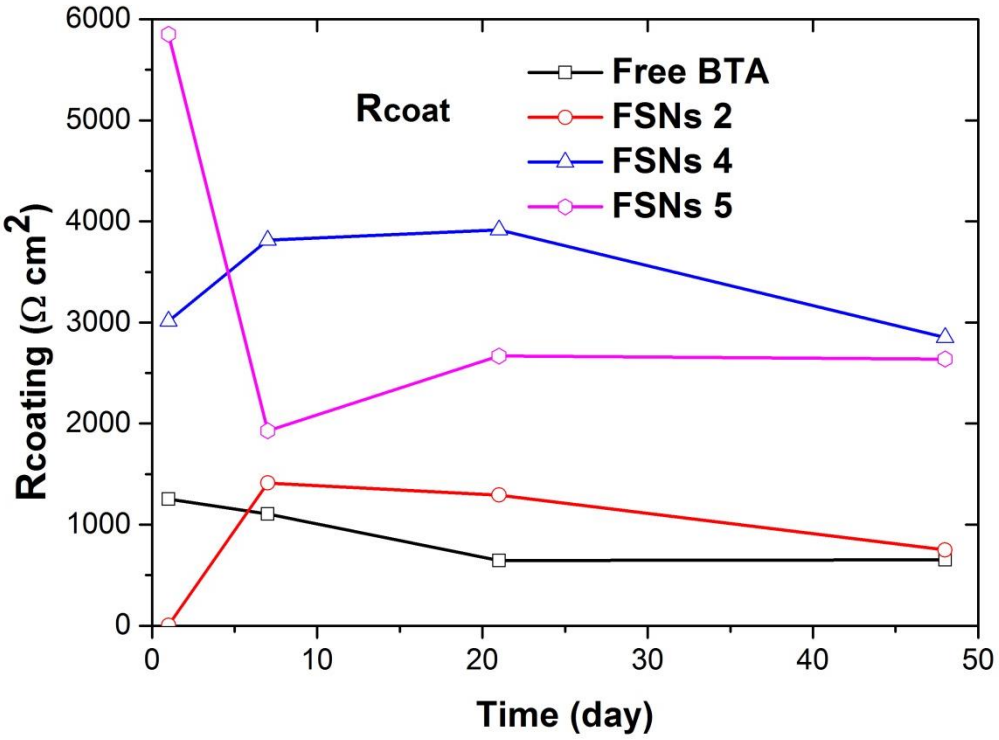

Figure S8. Calculated data for the Coating resistance (*R*coat) obtained by fitting of the EIS spectra using the equivalent circuit shown in Figure 8b.

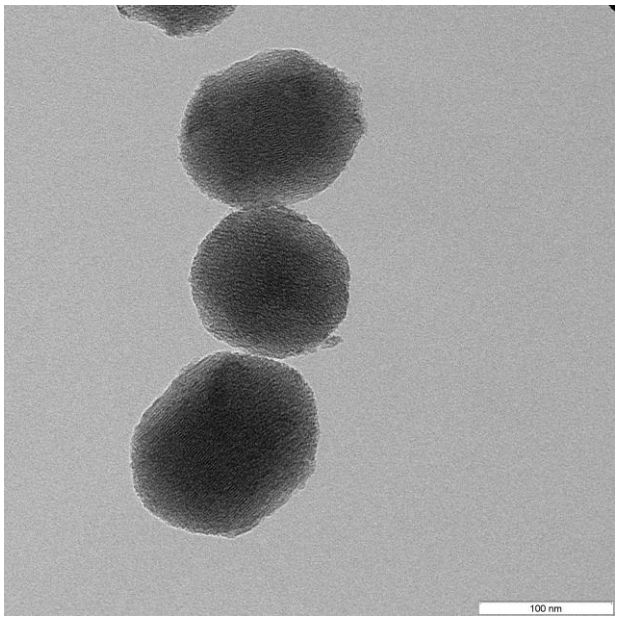

Figure S9. TEM image of capped loaded **FSN**s **5** after base-stimulated release measurement.

References

(1) Angelos, S.; Khashab, N. M.; Yang, Y. W.; Trabolsi, A.; Khatib, H. A.; Stoddart, J. F. and Zink, J. I. pH Clock-Operated Mechanized Nanoparticles. *J. Am. Chem. Soc.* **2009**, *131*, 12912-12914.
(2) Zheng, Z.; Huang, X.; Schenderlein, M.; Borisova, D.; Cao, R.; Möhwald, H. and Shchukin, D. Self-Healing and Antifouling Multifunctional Coatings Based on pH and Sulfide Ion Sensitive Nanocontainers. *Adv. Funct. Mater.* **2013**, *23*, 3307-3314.
(3) Borisova, D.; Möhwald, H. and Shchukin, D. G. Mesoporous Silica Nanoparticles for Active Corrosion Protection. *Acs Nano* **2011**, *5*, 1939-1946.
(4) Fung, B. M.; Khitrin, A. K. and Ermolaev, K. An Improved Broadband Decoupling Sequence for Liquid Crystals and Solids. *J. Magn. Reson.*, **2000**, *142*, 97-101.
(5) Morcombe, C. R.; Zilm, K. W. Chemical Shift Referencing in MAS Solid State NMR. *J. Magn. Reson.* **2003**, *162*, 479-486.
(6) Shchukin, D. G.; Grigoriev, D. O. and Möhwald, H. Application of Smart Organic Nanocontainers in Feedback Active Coatings. *Soft Matter*, **2010**, *6*, 720-725.
(7) Zheng, Z.; Huang, X.; Shchukin, D. A Cost-Effective pH-Sensitive Release System for Water Source pH Detection. *Chem. Commun.* **2014**, *50*, 13936-13939.
(8) DeMuth, P.; Hurley, M.; Wu, C.; Galanie, S.; Zachariah, M. R. and DeShong, P. Reversible Sorption of Water in the Crystalline Microporous Semiconductor K-SBC-1. *Microporous Mesoporous Mater.* **2011**, *141*, 128-131.